Semiautomated and automated algorithms for analysis of the carotid artery wall on computed tomography and sonography: a correlation study.

Semi-automated and automated Algorithms for the analysis of carotid artery wall in CT and Ultrasound: A correlation Study

ABSTRACT

Purpose: The characteristics and the thickness of the carotid wall may represent a parameter for the cerebrovascular risk stratification. The purpose of this study was to compare automated and semi-automated algorithms for the analysis of carotid artery wall thickness (CAWT) and intima-media thickness (IMT) in CT and Ultrasound respectively and studying the co-relation between them.

Material and Methods: Twenty consecutive patients underwent MDCTA and ultrasound analysis of carotid arteries (mean age 66 years; age range 59–79 years). The IMT of the 42 carotids was measured with novel and dedicated automated software analysis (called AtheroEdge™**,** Biomedical Technologies, Denver, CO, USA) and by four observers that manually calculated the IMT using ImgTracer™. The CAWT was automatically estimated using Athero-CTview™ and also semi-automatically quantified using ImgTracer™. The correlation between groups was calculated by using the Pearson rho statistic and the regression scatter plots were calculated. We evaluated inter-method agreement using a Bland–Altman analysis.

Results: All the techniques showed a strong correlation between them with the highest values obtained by the association between CAWT and IMT analysis (Pearson Rho = 0.9 with Confidence Interval from 0.82 to 0.95 and a *p-value* of 0.0001). The lowest value was obtained by the association between semi-automated US-IMT and automated CT-CAWT analysis (Pearson Rho = 0.44 with Confidence Interval from 0.15 to 0.66 and a *p-value* of 0.0047). In

the Bland-Altman analysis the better results were obtained by comparing the semi-automated and automated algorithm for the study of IMT with an interval from -16.1% to + 43.6%.

Conclusions: The results of this preliminary study demonstrated that the CAWT (Athero-CTView™) and IMT (AtheroEdge™) can be studied with this kind of software although the CT analysis need to be further improved.

Introduction

Atherosclerosis of the carotid artery represents a major risk factor in the development of stroke[1,2]. Although atherosclerosis can remain below the clinical horizon for a long time, it can manifest clinically as acute vascular disease at almost any stage of the disease process. Evaluation of atherosclerosis by means of clinical end points-morbidity and mortality-requires large study populations and necessitates considerable human and financial resources.

The use of surrogate markers to measure atherosclerosis burden in vivo has become wide spread. Imaging modalities have been developed to assess atherosclerosis in vivo in the arterial wall and B-mode ultrasonographic imaging of the carotid arterial walls occupies a unique position in atherosclerosis research[3,4]. This method enables sensitive, reproducible and non-invasive assessment of intima–media thickness (IMT) as a continuous variable. Epidemiological and clinical trial evidence as well as digitization and standardization have made carotid IMT a validated and accepted marker for generalized atherosclerosis burden and vascular disease risk[5,6,7].

Clinically, the IMT is usually measured by using ultrasound imaging. Longitudinal B-Mode projections of the artery are acquired and sonographers manually measure the IMT value by placing two markers on the distal wall, one in correspondence of the lumen-intima (LI) and

another in correspondence of the media-adventitia (MA) transitions; the IMT value is then computed as the Euclidean distance between the two markers[8,9,10].

The potentialities and diagnostic applications of multi-detector row CT angiography (MDCTA) have widely improved because of their high spatial and temporal resolution, the use of fast contrast material injection rates and post-processing tools. Besides stenosis degree, MDCTA clearly depicts carotid arterial wall thickness (CAWT) as recently demonstrated by *Saba et al*[11,12,13].

The purpose of this study was to compare semi-automated and automated algorithms for the analysis of CAWT and IMT.

MATERIALS AND METHODS

Demographic data. We retrospectively studied 20 patients, (13 males, 7 females; average age 66 years; age range 59–79 years) that underwent both MDCTA and Colour Doppler ultrasound (CD-US). MDCTA was performed every time a previous Colour Doppler ultrasound (CD-US) examination had evidenced a stenosis > 50% (according to NASCET criteria) and/or a plaque alteration (irregular plaque surface, ulcerated plaque). MDCTA was also performed when CD-US provided insufficient information about stenosis degree and plaque morphology, *i.e.*, in those patients with difficult necks (obese subjects, edema), large calcified plaques with acoustic shadowing or high carotid bifurcation.

Exclusion criteria for the study consisted of contraindications to iodinated contrast media, such as a known allergy to iodinated contrast materials or elevated renal function tests. Since imaging undertaken was not additional to that performed routinely in this group of patients, it is the policy of our divisional research committee that specific ethical approval did

not need to be obtained. Patients belonging to the study group were, however, asked to sign a written consent to perform MDCTA and CD-US. The department committee approved the study. Part of this study population was already used for other papers [**Blinded for Peer Review**].

CD-US technique. Colour duplex ultrasound scanning was performed by using a previously described technique [**Blinded for peer review**] with a US machine (Esaote MyLab™ 70, Milan, Italy) with a 10 MHz linear-array transducer. The carotid arteries were scanned, and tape recordings of vessel walls were recorded. No specific rules concerning gain controls settings were imposed to the sonographer, who was allowed to regulate gain controls according to their experience. We considered a blood flow velocity > 1.2 m/s as defining a NASCET stenosis with 50% lumen diameter reduction. The subject's head was tilted to get to the CCA just proximal to the bulb placed horizontally across the screen.

MDCTA technique. All patients underwent MDCTA of the supra-aortic vessels by using a previously described technique [**Blinded for peer review**] using a 16-detector row CT system (Philips Brilliance, Rotterdam, Netherlands). A basal scan was performed and was followed by the angiographic phase in which 80 mL of contrast medium (Iomeron 400; Bracco, Milan, Italy) were injected into a cubital vein, using a power injector at a flow rate of 5 mL/s and an 18-gauge intravenous catheter. A bolus tracking technique was used to calculate the correct timing of the scan. Dynamic monitoring scanning began 6 seconds after the beginning of the intravenous injection of contrast material. The trigger threshold inside the ROI was set at + 80 HU above the baseline. The delay between the acquisitions of each monitoring scan was

one second. When the threshold reached the patient was instructed not to breathe and after an interval of four seconds the scan started in the caudo-cranial direction. CT technical parameters included: matrix 512x512, field of view (FOV) 14–19 cm; mAs 180–200; kV 120–140; section thickness 1 mm, increment 0.5 mm and the window was selected according to previous papers[20]. Angiographic acquisition included the carotid siphon. None of the patients included in the study had a medical history of cardiac output failure, or any contraindications to iodinated contrast media.

None of the patients included in the study had a medical history of cardiac output failure, any contraindications to iodinated contrast media, such as a known allergy to iodinated contrast media or elevated renal function tests.

Automated algorithm for the CAWT analysis. We use Athero-CTview™ for computation of the CAWT in CT images. Variational level set method (VLSM) without-re-initialization[14] was used in the study for arterial wall segmentation with CT images of carotid arteries. The details regarding VLSM can be found in the appendix. Wall thickness measured by polyline distance[15] was calculated for each carotid artery section, defined as the closest average distance from the estimated lumen boundary to the outer wall boundary[15] (**Figure 1**).

In this study we explored as anatomical range from 2-3 cm below the bifurcation to 2-3 cm in the ICA.

Automated algorithm for the IMT analysis. The concept of automated IMT measurement based on edge estimation for LI and MA borders using a two stage process was first published by *Molinari et al*[16] as AtheroEdge™ first published as CAMES (Completely

Automated Multi-resolution Edge Snapper). The principal advantages of this system are: (a) full automation; (b) border estimation of lumen-intima (LI) and media-intima (MA). The AtheroEdge™ architecture consists of two stages: First stage is the recognition phase and second phase is the LI and MA boundary estimation and IMT measurement.

The sequence of steps for stage-I consists of (a) down sampling the original image to half its size and (b) reduction of speckle noise; the far and near wall edges of the artery are then computed by convolving the image with the first order Gaussian derivative with a priori scale (**Figure 2**). The scale of the Gaussian kernel is adjusted almost the same size as the wall thickness. Finally, the peak detection heuristics is adapted to yield the edge points. Stage-II of the overall system consists of an accurate edge-snapper based on first order absolute moments, well discussed in our recent work[17,18]. The LI and MA border detection in the region of interest is based on peak detection driven by Heuristics. The IMT was measured as the polyline distance metric[19] between the LI and MA border profiles.

Semi-automated (Ground Truth) assessment of CT and Ultrasound.

ImgTracer™ (Global Biomedical Technologies, Inc., California, USA) is a user-friendly interactive software system that was used for two purposes: (a) for tracing LI and MA borders and then computing the IMT in Ultrasound images; (b) tracing of carotid lumen and outer wall borders and computing the wall thickness (CAWT) in CT images. On invoking the ImageTracer™ software system, the user is prompted to select MR/CT package or Ultrasound package for ground truth tracing and semi-automated quantification. The tracing tool concept and foundation is same for Ultrasound and MR/CT, except for few differences: (a) In Ultrasound, the borders for LI/MA is traced without closing the borders (first and last point on

the curve), while the borders for the CT lumen/outer wall are automatically closed as soon as the last point is traced. The process of tracing has same foundation leading to CAWT in CT and IMT in ultrasound. With the click of the button, the physician can "load" the ultrasound DICOM or CT DICOM image in ImgTracer™ system. The user can automatically adjust the window/level of the image for the superior visualization of the atherosclerotic walls in CT/Ultrasound images. With the comfort of the "zoom" button, the physician can zoom the CT/Ultrasound image region where the ground truth borders need to be traced. This allows the physician or sonographer to trace the lumen-intima (LI) and media-adventita (MA) interfaces with the help of the "trace" button in ultrasound or lumen/outer wall borders in the CT image. The "trace" menu has different options such as selection of left or right carotids, spline-fitted smooth borders vs piece-wise polyline borders and closed vs. unclosed borders. In CT package of ImgTracer™, the output of the tracing process automatically closes the contours around the lumen or outer wall. In case of Ultrasound, the LI/MA borders are never closed. Using the right combination protocol, the physician can generate the smooth LI and MA arterial wall borders in Ultrasound by clicking few set of points (say 10 to 15) along the whole artery in the selected region. A similar process is applied for CT lumen and outer wall in a clock-wise or anti-clockwise fashion. The physician or sonographer has an option to select manually the IMT zone in Ultrasound image which is one to two centimetres from the shoulder of the carotid bulb. In the CT image, the radiologist has an option to zoom or unzoom to accurately trace the lumen/outer wall borders. The protocol is user friendly and the uses left click mouse to trace the LI and MA borders in Ultrasound (lumen/outer wall in CT) and right click to end the tracing process for a particular image frame. ImgTracer™ has a general tool that allows the physician to save the borders as set of points in a boundary text file or can save the borders on

the image as an overlay. This overlay image can be saved in DICOM, JPEG, TIFF or BMP formats. The most important feature of ImgTracer™ is the ability to automatically compute the IMT values (or CAWT values) once the physician has traced the LI and MA borders or lumen/outer wall borders in CT. Standard algorithm earlier published by Suri *et al*. was adapted in IMT/CAWT computation and now used by several groups around the world[33,34] . The ImgTracer™ can allow multiple users to tracer the manual carotid far walls and compare them eventually with different colour codes on the image. This is very useful feature to see the variability effect of different observers on the same carotid image. **Figure 3** shows examples of manual tracings by using ImgTracer™.

Statistical analysis. Kolmogorov-Smirnov *Z* test for the distribution the normality of each continuous variable group was calculated. Continuous data were described as the mean value ± Standard Deviation (SD). The correlation between groups was calculated by using the Pearson rho statistic and the regression scatter plots were calculated. We evaluated inter-method agreement using a Bland–Altman analysis. A *p*-value less than 0.05 were considered significant. *R* software (www.r-project.org) was employed for statistical analyses.

Results

General Analysis. The summary statistics of the CAWT and IMT measurements are provided in the **Table 1**. In the CT groups the Kolmogorov-Smirnov *Z* test demonstrated the normality of the distribution whereas in the ultrasound groups the the Kolmogorov-Smirnov *Z* test did not show a normal distribution. The Box-and-Whiskers plots are given in **Figure 4**.

Correlation analysis. The correlation analysis is summarized in the **Table 1** whereas the scatter-plots are given in **Figure 5**. All the techniques showed a strong correlation between them with the highest values obtained by the association between semi-automated and Ground Truth automated US-IMT analysis (Pearson Rho = 0.9 with Confidence Interval from 0.82 to 0.95 and a p value of 0.0001). The lowest value was obtained by the association between Ground Truth IMT and semi-automated CT-CAWT analysis (Pearson Rho = 0.44 whit Confidence Interval from 0.15 to 0.66 and a p value of 0.0047).

Bland Altman analysis. We evaluated the performance of the semi-automated and automated algorithms in the quantification of CAWT and IMT by using also the Bland-Altman statistics and the results are give in the **Figure 6**. The better results were obtained by comparing the semi-automated and automated algorithm for the study of IMT with an interval from -16.1% to + 43.6% whereas sub-optimal results where detected between automated algorithm for the study of CAWT versus automated algorithm for the study of IMT with an interval from -16.1% to + 43.6%.

DISCUSSION

In the last years, several papers have demonstrated that the thickness of the carotid wall, measured by using the ultrasound (the analysis of IMT) or by using the Computed Tomography (the analysis of CAWT) is associated to an increase of cerebrovascular risk, as well as to several metabolic and neurological pathologies[6,8,9,10,11,12,13]. Nowadays the assessment of IMT represent an important step in the cardiovascular risk analysis because it is considered a reliable indicator of cardiovascular and cerebrovascular risk[21] and the Rotterdam study showed that the IMT had an important diagnostic and predictive value for incident myocardial infarction[22].

Recently, much attention has been given to the association between ultrasound measurement of the IMT and the Framingham risk scores[24]. Polak *et al.*[24] showed that the Framingham risk factors accounted only for about 28% of the common and internal carotid IMT variability and concluded that the IMT predicting value should be further compared in outcome studies. In another study, the same team compared manual IMT measurements from ultrasound images to measurements obtained through an automated computer program[25] and demonstrated that the obtained IMT values maintained the same correlation with the cardiovascular risks. Thus, they concluded that the computer measurements of the IMT could be used in large studies as surrogate for manual measurements.

This study represents a further step in the analysis of human and computer based measurements to be used in large and multi-centre trials. We widened the analysis to comprise CT and US based IMT measurements. Several recent publications[26,27,28,29] have proposed semi-automated and automated techniques in the analysis on the IMT, but on the best of our knowledge no papers were published about automatic and semi-automatic algorithms in the CAWT quantification by using CT. The purpose of this study was to compare automated and semi-automated algorithms for the analysis of CAWT and IMT.

By analyzing the IMT and CAWT values we observed that there is a statistically significant difference ($p = 0.001$) between the IMT values (both automated and semi-automated) and the automated CAWT values whereas no statistically significant difference was present between the IMT automated and semi-automated techniques. This data should not surprise because it reflects that the IMT technique algorithm are nowadays extremely advanced because these were extensively analysed in the last ten years. The algorithms for the study of CAWT are new and should be tested to refine their potentialities. The mean CAWT value

obtained with the semi-automatic algorithm was 1.01 mm that is markedly lower compared to the automated CAWT values and IMT values (automated and semi-automated). This was an unexpected results because in previous papers it was reported that the CAWT value is bigger that the IMT[12] and should be tested in further publications.

The correlation analysis demonstrated the techniques showed a strong correlation between all the algorithms with the highest value obtained by the association between semi-automated and automated Ultrasound-IMT analysis (Pearson Rho = 0.9 whit Confidence Interval from 0.82 to 0.95 and a p value of 0.0001). The lowest value was obtained by the association between semi-automated Ultrasound-IMT and automated CT-CAWT analysis (Pearson Rho = 0.44 whit Confidence Interval from 0.15 to 0.66 and a p value of 0.0047).

In the Bland-Altman analysis the better results were obtained by comparing the semi-automated and automated algorithm for the study of IMT with an interval from -16.1% to + 43.6% whereas sub-optimal results where detected between automated algorithm for the study of CAWT versus automated algorithm for the study of IMT with an interval from -16.1% to + 43.6%. The IMT algorithms show very good results whereas the CAWT algorithms show sub-optimal results.

In this study there is a limitation: this is a retrospective analysis. Further to this point, we used the same techniques, hardware, operators and data standardization and so the variability in the retrospective analysis should have been reduced but these results should be further tested in a prospective study.

CONCLUSION

In conclusion, the algorithms for the automated and semi-automated study of carotid artery wall are becoming a reality that in the future can be implemented in the clinical daily activity. The results of this preliminary study demonstrated that the CAWT and IMT can be studied with this kind of software although the CT analysis need to be further improved.

Appendix

The evolution equation of the traditional level set formulation can be written in the following general form[27],

$$\frac{\partial \varphi}{\partial t} + F\left|\nabla \varphi\right| = 0 \tag{1}$$

F is the speed function, which is depended on the imaging data and level set function φ. The moving front C can be represented by the zero level set as $C(t) = \{(x, y) \mid \varphi(t, x, y) = 0\}$. We will limit our problem domain in two-dimension image space.

For traditional LSM[28], φ is required to be kept close to a signed distance function during the evolution, therefore re-initialization is required constantly during the evolution. However the re-initialization procedure can be very complicated and time consuming, and have great side effects. In order to overcome those difficulties, the evolution equation 1 is redefined as

$$\frac{\partial \varphi}{\partial t} + \frac{\partial \varepsilon}{\partial \varphi} = 0 \tag{2}$$

$$\varepsilon(\varphi) = \mu \int_{\Omega} \frac{1}{2}(\left|\nabla \varphi\right| - 1)^2 dxdy + \lambda \int_{\Omega} g\delta(\varphi)\left|\nabla \varphi\right| dxdy + \nu \int_{\Omega} gH(-\varphi)dxdy \tag{3}$$

The first term in the right hand side of equation 3 is the measurement of the distance of how close a function φ is to a signed distance function, this term will eliminate the re-initialization of φ during level set evolution, and μ>0, controlling the weight of the penalty term. The second and third terms in the right hand side of equation 3 are the energy terms which will drive the motion of the zero level curve of φ to the desired boundaries. λ>0 and ν is a constant, δ is a univariate Dirac function, H is the Heaviside function, g is the edge indicator function defined as:

$$g = \frac{1}{1+\left|\nabla G_\sigma * I\right|^2} \tag{4}$$

G_σ is the Gaussian kernel with given σ , I is the given image matrix.

Finally, equation 3 can be solved as:

$$\frac{\partial \varphi}{\partial t} = \mu[\Delta\varphi - div(\frac{\nabla\varphi}{\left|\nabla\varphi\right|})] + \lambda\delta(\varphi)div(g\frac{\nabla\varphi}{\left|\nabla\varphi\right|}) + \nu g\delta(\varphi) \tag{5}$$

Equation 5 can now be easily implemented by simple finite difference scheme. The proposed VLSM was implemented in Matlab (MathWorks, Natick, MA). The segmentation procedure was done on a slice-by-slice basis as follows: (1) initializing boundary inside lumen by a region growing method with a manually selected point inside the lumen. (2) The initial boundary evolved according to Equation 5, and stop at the luminal boundary. Usually the iteration is chosen to be 100 to ensure the initial boundary will evolve towards luminal boundary as close as possible. (3)The segmented lumen boundary grows outward by 2 pixels for the initialization of outer wall boundary segmentation. (4) Based on step 3, the newly initialized boundary will evolve similar as in step 2 according to Equation 5. Due to poor contrast between outer wall and surrounding tissues, usually 20 iteration steps were chosen in order to avoid over-estimation.

References

1) Gorelick PB. Stroke Prevention Therapy Beyond Antithrombotics: Unifying Mechanisms in Ischemic Stroke Pathogenesis and Implications for Therapy. Stroke 2002;33:862-875.

2) Sacco RL, Adams R, Albers. Guidelines for Prevention of Stroke in Patients With Ischemic Stroke or Transient Ischemic Attack. Stroke 2006;37:577-617.

3) Iglesias del Sol A, Bots ML, Grobbee DE, Hofman A, Witteman JC. Carotid intima-media thickness at different sites: relation to incident myocardial infarction; The Rotterdam Study. Eur Heart J 2002; 23: 934-940.

4) Kitamura A, Iso H, Imano H, Ohira T, Okada T, Sato S, Kiyama M, Tanigawa T, Yamagishi K, Shimamoto T. Carotid intima-media thickness and plaque characteristics as a risk factor for stroke in Japanese elderly men. 2004;35:2788-2794.

5) Bonithon-Kopp C, Touboul PJ, Berr C, Leroux C, Mainard F, Courbon D, Ducimetie`re P. Relation of intima-media thickness to atherosclerotic plaques in the carotid arteries: the EVA study. Arterioscler Thromb Vasc Biol 1996;16:310-316.

6) Ebrahim S, Papacosta O, Whincup P, Wannamethee G, Walker M, Nicolaides AN, Dhanjil S, Griffin M, Belcaro G, Rumley A, Lowe GDO. Carotid plaque, intima media thickness, cardiovascular risk factors, and prevalent cardiovascular disease in men and women: the British Regional Heart Study. Stroke 1999;30:841- 850.

7) Salonen JT, Salonen R. Ultrasonographically assessed carotid morbidity and the risk of coronary heart disease. Arterioscler Thromb 1991;11:1245-1249.

8) Hodis HN, Mack WJ, Barth J. Carotid intima-media thickness as a surrogate end point for coronary artery disease. Circulation 1996; 94: 2311-2.

9) Ellis SM, Sidhu PS. Granularity of the carotid artery intima-medial layer: reproducibility of quantification by a computer-based program. Br J Radiol 2000; 73: 595-600.

10) Burke GL, Evans GW, Riley WA, Sharrett AR, Howard G, Barnes RW, Rosamond W, Crow RS, Rautaharju PM, Heiss G. Arterial wall thickness is associated with prevalent cardiovascular disease in middle-aged adults. The Atherosclerosis Risk in Communities (ARIC) Study. Stroke 1995; 26: 386-91.

11) Saba L, Sanfilippo R, Pascalis L, Montisci R, Caddeo G, Mallarini G. Carotid artery wall thickness and ischemic symptoms: evaluation using multi-detector-row CT angiography. Eur Radiol 2008; 18: 1962-71.

12) Saba L, Sanfilippo R, Montisci R, Mallarini G. Carotid artery wall thickness: comparison between sonography and multi-detector row CT angiography. Neuroradiology 2010; 52: 75-82.

13) Saba L, Sanfilippo R, Montisci R, Mallarini G. Associations between carotid artery wall thickness and cardiovascular risk factors using multidetector CT. AJNR Am J Neuroradiol 2010; 31: 1758-63.

14) Li C, Xu C, Gui C, Fox M. Level set evolution without re-initialization: A new variational formulation. CVPR, 2005

15) Suri JS, Haralick RM, Sheehan FH. Greedy algorithm for error reduction in automatically produced boundaries from low contrast ventriculograms. International Journal of Pattern Analysis and Applications 2000; 3:39-60.

16) Molinari F, Loizou C, Zeng G, Pattichis C, Chandrashekar D, Pantziaris M, et al. Completely Automated Multi-Resolution Edge Snapper (CAMES) - A New Technique for an Accurate Carotid Ultrasound IMT Measurement and its Validation on a Multi-Institutional Database. SPIE Medical Imaging Conference. Lake Buena Vista (Orlando), FL, USA, 2011 (In Press).

17) Demi M, Paterni M, Benassi A. The first absolute central moment in low-level image processing. Comput Vis Image Und. 2000;80:57-87.

18) Faita F, Gemignani V, Bianchini E, Giannarelli C, Ghiadoni L, Demi M. Real-time measurement system for evaluation of the carotid intima-media thickness with a robust edge operator. J Ultrasound Med. 2008;27:1353-61.

19) Suri, JS., Haralick, RM, Sheehan FH. Greedy algorithm for error correction in automatically produced boundaries from low contrast ventriculgrams; Pattern Analysis and Applications: 2000; 3:39-60.

20) Saba L, Mallarini G. MDCTA of carotid plaque degree of stenosis: evaluation of interobserver agreement. AJR Am J Roentgenol 2008; 190: W41-6.

21) Simon A, Gariepy J, Chironi G et al. Intima-media thickness: a new tool for diagnosis and treatment of cardiovascular risk. **J Hypertens 2002;20:159-69**.

22) van der Meer IM, Bots ML, Hofman A, et al. Predictive value of noninvasive measures of atherosclerosis for incident myocardial infarction: the Rotterdam Study. **Circulation 2004;109:1089-94**.

23) Loizou CP, Pattichis CS, Nicolaides AN, Pantziaris M. Manual and automated media and intima thickness measurements of the common carotid artery. IEEE Trans Ultrason Ferroelectr Freq Control 2009; 56 (5): 983-94

24) Polak JF, Pencina MJ, Meisner A, Pencina KM, Brown LS, Wolf PA, D'Agostino RB, Sr.: Associations of carotid artery intima-media thickness (imt) with risk factors and prevalent cardiovascular disease: Comparison of mean common carotid artery imt with maximum internal carotid artery IMT. **J Ultrasound Med** 2010;29:1759-1768.

25) Polak JF, Pencina MJ, Herrington D, O'Leary DH: Associations of edge-detected and manual-traced common carotid intima-media thickness measurements with framingham risk factors: The multi-ethnic study of atherosclerosis. **Stroke** 2011;42:1912-1916.

26) Ilea DE, Whelan PF, Brown C, Stanton A. An automatic 2D CAD algorithm for the segmentation of the IMT in ultrasound carotid artery images. Conf Proc IEEE Eng Med Biol Soc 2009; 2009 (): 515-9.

27) Molinari F, Zeng G, Suri JS. Intima-media thickness: setting a standard for a completely automated method of ultrasound measurement. IEEE Trans Ultrason Ferroelectr Freq Control 2010; 57: 1112-24

28) Molinari F, Zeng G, Suri JS. A state of the art review on intima-media thickness (IMT) measurement and wall segmentation techniques for carotid ultrasound. Comput Methods Programs Biomed 2010; 100: 201-21.

29) Osher S, Sethian JA. Fronts propagating with curvature dependent speed: algorithms based on Hamilton-Jacobi formulations. J. Comp. Phys. 1998;79:12-49.

30) Jasjit S. Suri, Kecheng Liu, Sameer Singh, Swamy N. Laxminarayan, , Xiaolan Zeng, and Laura Reden, Shape Recovery Algorithms Using Level Sets in 2-D/3-D Medical Imagery: A State-of-the-Art Review, IEEE TRANSACTIONS ON INFORMATION TECHNOLOGY IN BIOMEDICINE, VOL. 6, NO. 1, MARCH 2002: 8-28.

Tables

Table 1 : summary statistics table										
	Mean	Variance	SD	SEM	Median	95% CI	Minimum	Maximum	5 - 95% Percentile	Normal Distr. K-S Z-test
Automated US IMT	1,628	0,4928	0,702	0,111	1,543	1,266 - 1,667	0,639	4,225	0,780 - 2,860	**0,001***
Ground Truth US IMT	1,403	0,3188	0,5647	0,0893	1,237	1,093 - 1,515	0,703	3,086	0,742 - 2,715	**0,001***
Semi-Automated CT CAWT	1,547	0,085	0,2915	0,0461	1,532	1,396 - 1,661	0,983	2,299	1,049 - 1,944	0,778
Ground Truth CT CAWT	1,01	0,1071	0,3272	0,0517	0,949	0,822 - 1,153	0,545	1,814	0,559 - 1,652	0,205

* = statistically significant p value.

Table 2: correlation analysis				
Method	**Ground Truth CAWT**	**Automated CAWT**	**Ground Truth IMT**	**Automated IMT**
Ground Truth CT CAWT	**NC**	0,58 (0,33-0,75) p value = 0,0001	0,61 (0,37 - 0,77) p value = 0,0001	0,63 (0,39 - 0,78) p value = 0,0001
Automated CT CAWT	0,58 (0,33-0,75) p value = 0,0001	**NC**	0,44 (0,15 - 0,66) p value = 0,0047	0,47 (0,18 - 0,68) p value = 0,0023
Ground Truth US IMT	0,61 (0,37 - 0,77) p value = 0,0001	0,44 (0,15 - 0,66) p value = 0,0047	**NC**	0,9 (0,82 - 0,95) p value = 0,0001
Automated US IMT	0,63 (0,39 - 0,78) p value = 0,0001	0,47 (0,18 - 0,68) p value = 0,0023	0,9 (0,82 - 0,95) p value = 0,0001	**NC**

Between parentesis 95% Confidence interval

Figures

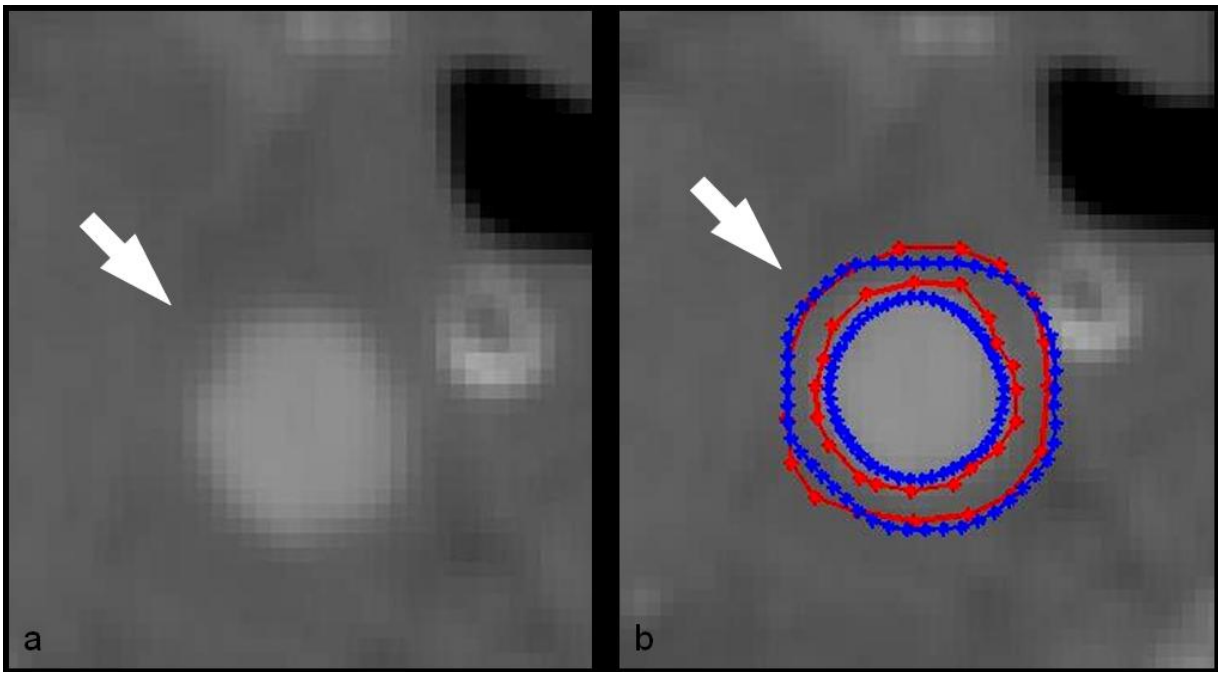

Fig 1. MDCTA axial image original slice (**a**) and after manual and automated detection (**b**). White arrows indicate the internal carotid artery. In panel b are visible the detected boundaries using **Athero-CTview™** (blue) superimposed with manual tracing using **ImgTracer ™** (red). The tracked lumen and outer wall boundaries are well close to the manual tracing.

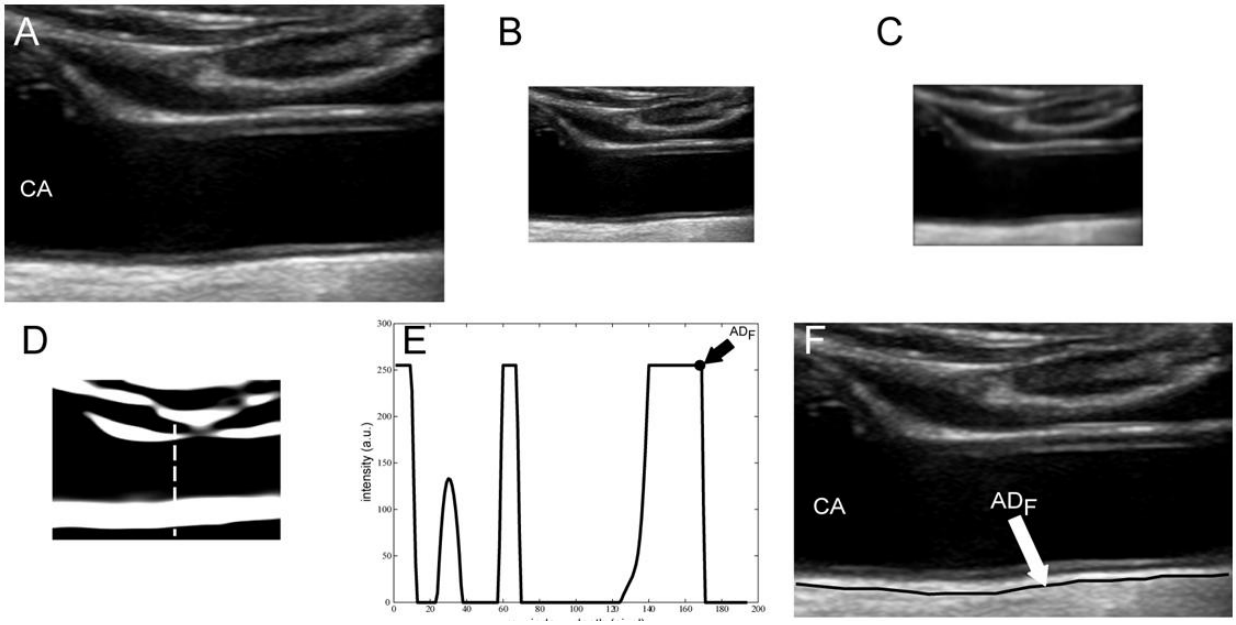

Fig 2. Far adventitia (AD_F) profile computation using AtheroEdge™: Original cropped image. **B**) Down sampled image. **C**) Despeckled image. **D**) Image after convolution with first-order Gaussian derivative (sigma = 8). If we take the intensity profile of the column (shown as white dotted line), one can obtain values equal to 255 that corresponds to arterial wall. **E**) Intensity profile of the column indicated by the vertical dashed line in panel **C**. (AD_F indicates the position of the far adventitia wall). **F**) Final AD_F profile.

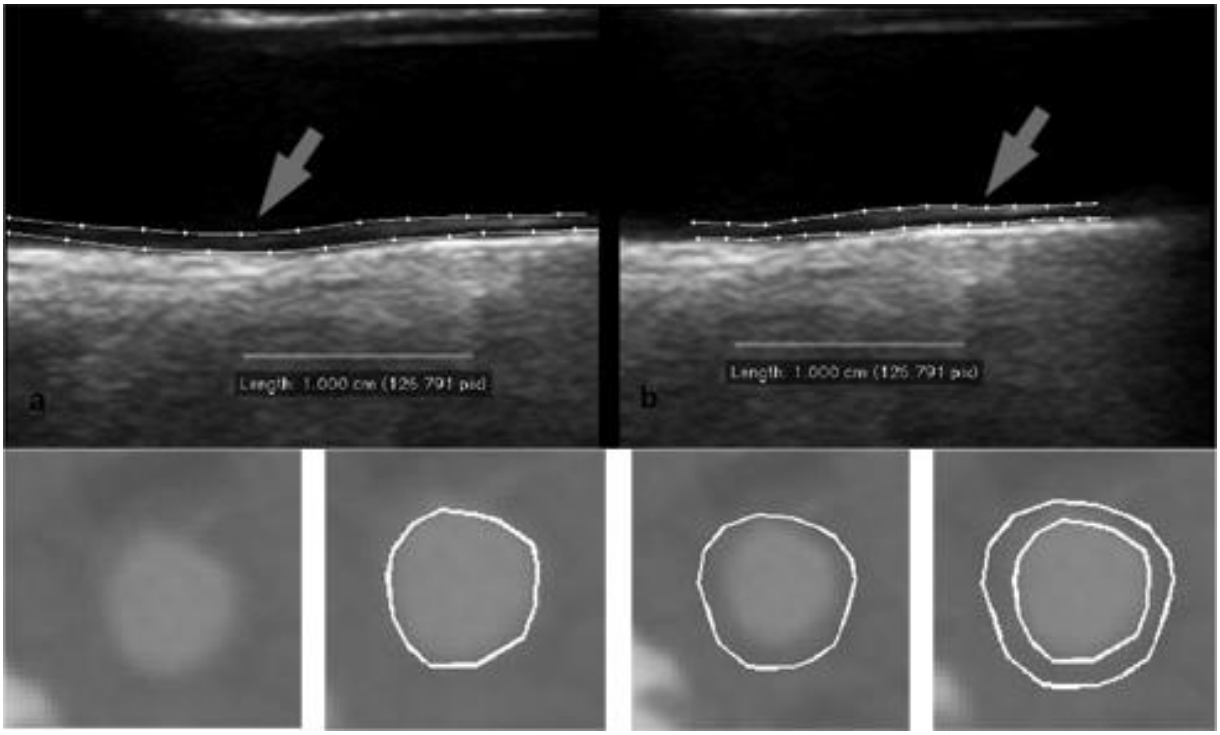

Fig 3. Manual delineation of the lumen-intima and media-adventitia interfaces by ImgTracer™ for Ultrasound and CT images. Top row: manual tracings of the lumen-intima (indicated by the arrows) and of the media-adventitia interfaces in two B-Mode ultrasound images. Bottom row: manual tracings in CT images. The manual delineation process is shown left to right: from the original image, first the lumen-intima profile is traced, then the media-adventitia. The rightmost panel shows the two profiles overlaid to the original CT image.

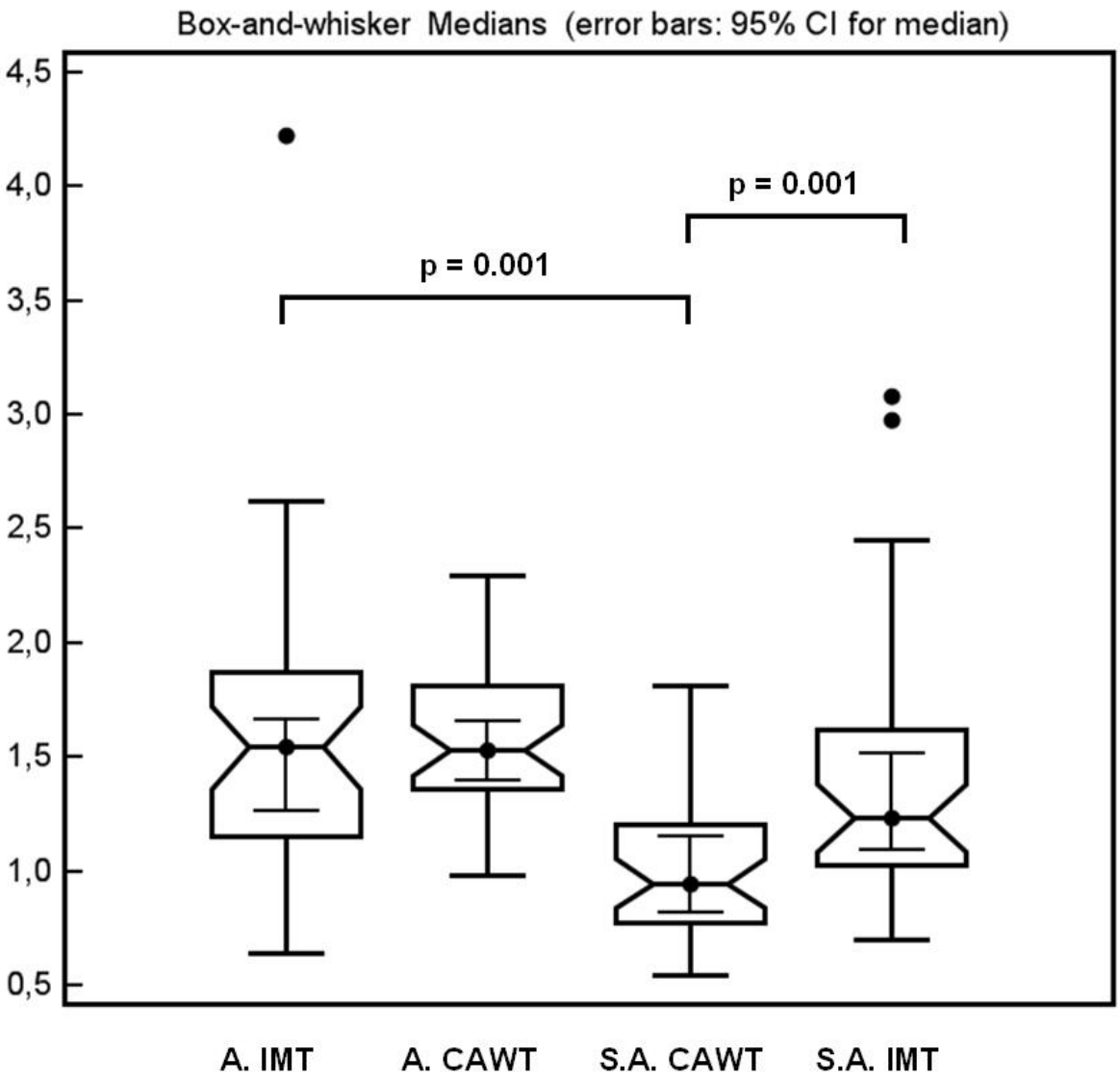

Fig 4. Box-and-Whisker plots of the IMT measurements. From left to right: automated IMT measurement by US; automated IMT measurement by CT; semi-automated IMT measurement by US, and semi-automated IMT measurement by CT. Each plot shows the median value, along with the first and third quartiles. The vertical error bars represent the 95% confidence interval. Each The black dots represent the outliers.

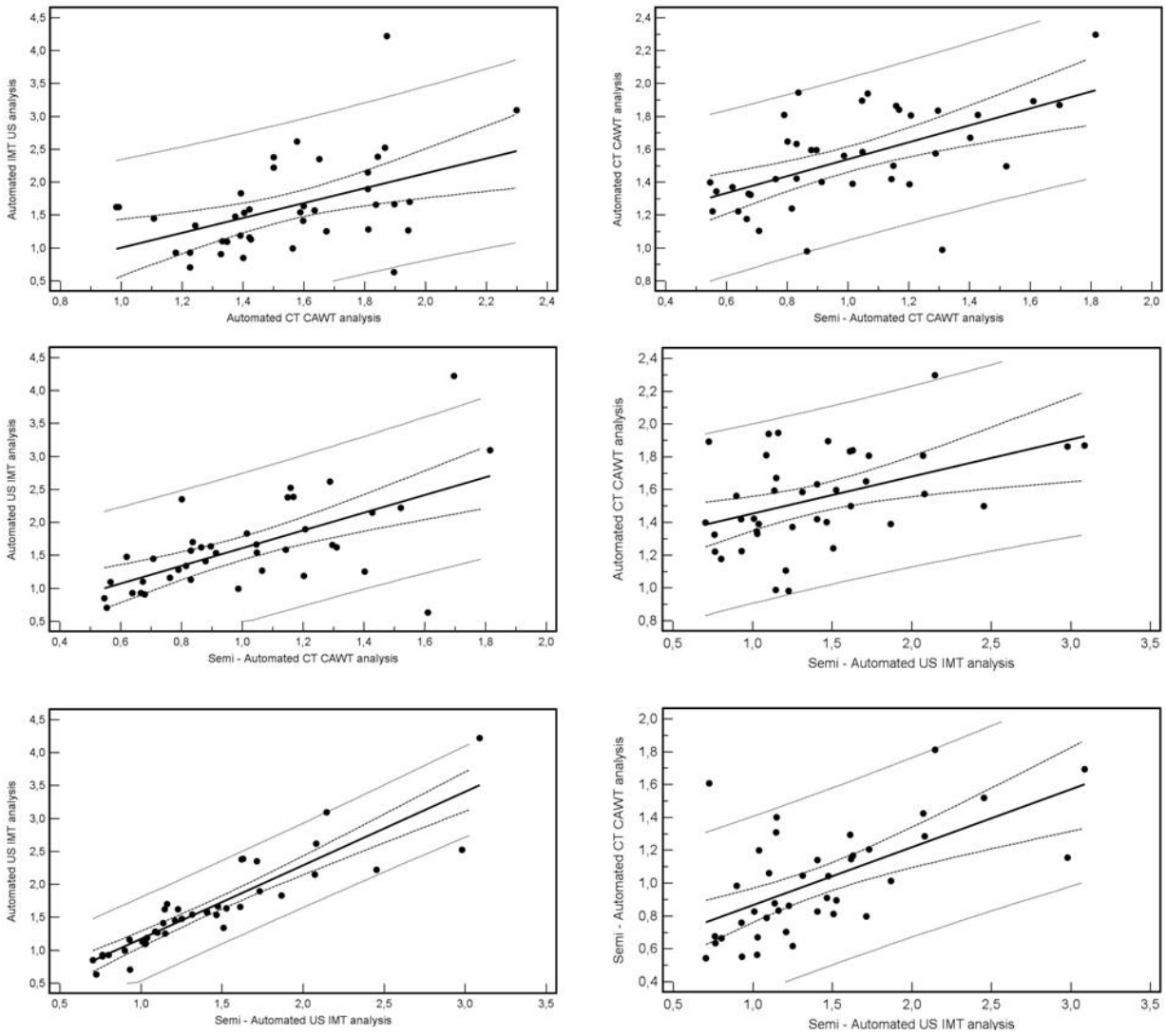

Fig 5. Scatter-plot analysis of the IMT measurements. The left column is relative to the automated US measurements (vertical axis) vs. automated CT (top), semi-automated CT (middle), and semi-automated US (bottom). The right column is relative to the automated CT measurements (vertical axis) vs. semi-automated CT (top) and vs. semi-automated US (middle). The bottom panel of the right column is relative to semi-automated CT vs. semi-automated US (bottom).

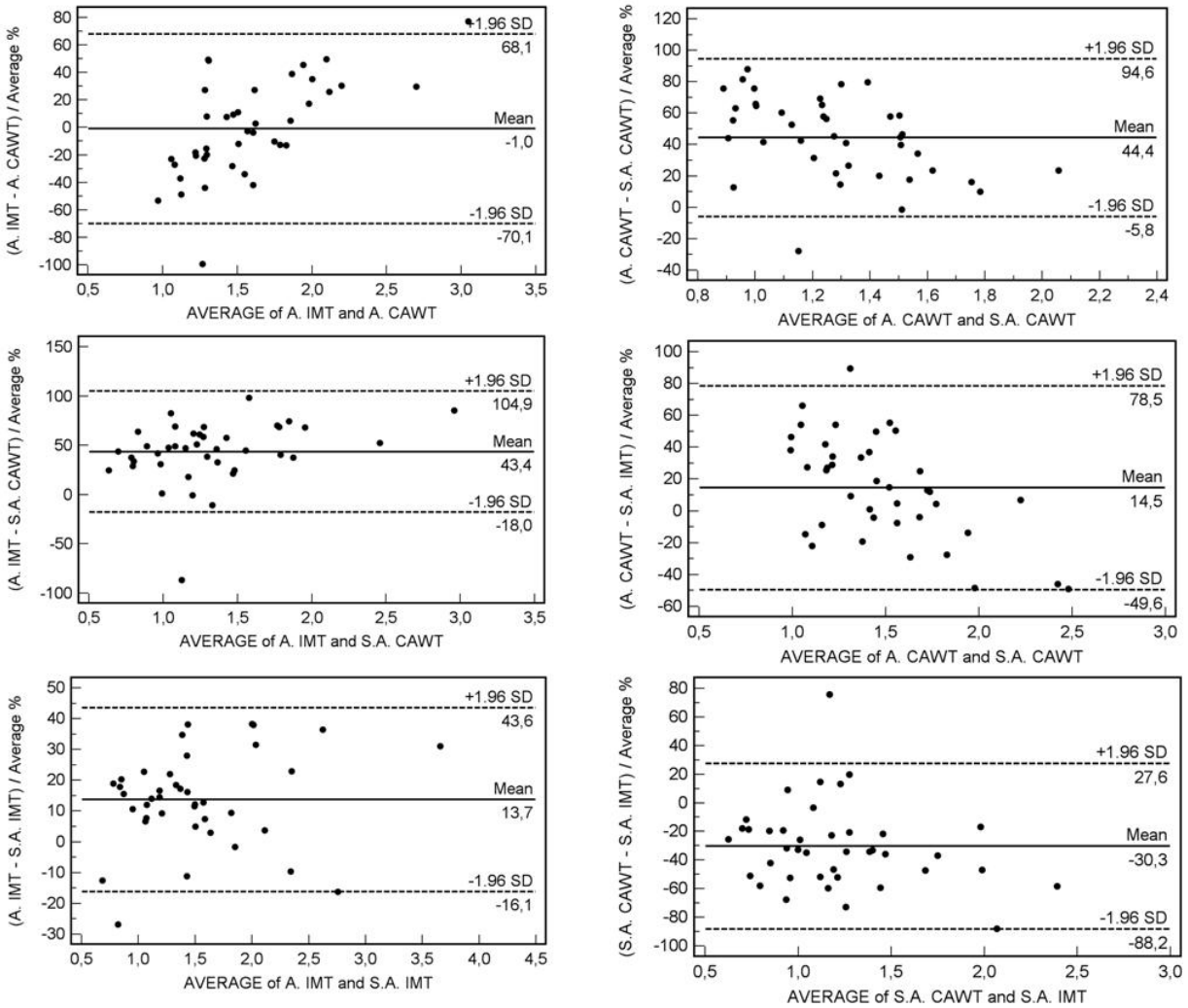

Fig 6. Bland Altman plots for the IMT measurements. The left column is relative to the automated US measurements (vertical axis) vs. automated CT (top), semi-automated CT (middle), and semi-automated US (bottom). The right column is relative to the automated CT measurements (vertical axis) vs. semi-automated CT (top) and vs. semi-automated US (middle). The bottom panel of the right column is relative to semi-automated CT vs. semi-automated US (bottom).